

Catalytic formation of C(sp³)-F bonds via heterogeneous photocatalysis

Giulia Tarantino, and Ceri Hammond

ACS Catal., Just Accepted Manuscript • Publication Date (Web): 20 Sep 2018

Downloaded from <http://pubs.acs.org> on September 20, 2018

Just Accepted

“Just Accepted” manuscripts have been peer-reviewed and accepted for publication. They are posted online prior to technical editing, formatting for publication and author proofing. The American Chemical Society provides “Just Accepted” as a service to the research community to expedite the dissemination of scientific material as soon as possible after acceptance. “Just Accepted” manuscripts appear in full in PDF format accompanied by an HTML abstract. “Just Accepted” manuscripts have been fully peer reviewed, but should not be considered the official version of record. They are citable by the Digital Object Identifier (DOI®). “Just Accepted” is an optional service offered to authors. Therefore, the “Just Accepted” Web site may not include all articles that will be published in the journal. After a manuscript is technically edited and formatted, it will be removed from the “Just Accepted” Web site and published as an ASAP article. Note that technical editing may introduce minor changes to the manuscript text and/or graphics which could affect content, and all legal disclaimers and ethical guidelines that apply to the journal pertain. ACS cannot be held responsible for errors or consequences arising from the use of information contained in these “Just Accepted” manuscripts.



Catalytic formation of C(sp^3)-F bonds *via* heterogeneous photocatalysis

Giulia Tarantino^a and Ceri Hammond^{a*}

^aCardiff Catalysis Institute, Cardiff University, Park Place, Cardiff, CF10 3AT, UK

* hammondc4@cardiff.ac.uk; <http://blogs.cardiff.ac.uk/hammond/>

Abstract. Due to their chemical, physical and biological properties, fluorinated compounds are widely employed throughout society. Yet, despite their critical importance, current methods of introducing fluorine into compounds suffer from severe drawbacks. For example, several methods are non-catalytic, and employ stoichiometric equivalents of heavy metals. Existing catalytic methods, on the other hand, exhibit poor activity, generality, selectivity, and/or have not been achieved by heterogeneous catalysis, despite the many advantages such an approach would provide. Here we demonstrate how selective C(sp^3)-F bond synthesis can be achieved *via* heterogeneous photocatalysis. Employing TiO₂ as photocatalyst and Selectfluor® as mild fluorine donor, effective decarboxylative fluorination of a variety of carboxylic acids can be achieved in very short reaction times. In addition to displaying the highest turnover frequencies of any reported fluorination catalyst to date (up to 1050 h⁻¹), TiO₂ also demonstrates excellent levels of durability, and the system is catalytic in the number of photons required *i.e.* a photon efficiency greater than 1 is observed. These factors, coupled with the generality and mild nature of the reaction system, represent a breakthrough toward the sustainable synthesis of fluorinated compounds.

Keywords: fluorination • photochemistry • heterogeneous catalysis • spectroscopy • photocatalysis

Supporting Information is available.

Introduction

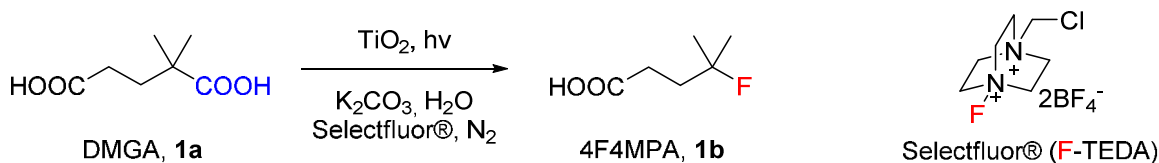
Increasing demand for fluorinated compounds, widely employed as pharmaceuticals, agrochemicals, materials¹ or tracers for Positron Emission Tomography (as ¹⁸F),² has prompted a surge of interest in the development of new strategies to perform selective fluorination. However, whilst many breakthroughs have been made,³ such as the development of safer electrophilic fluorinating agents such Selectfluor®, the selective and catalytic formation of C(*sp*³)-F bonds remains an immense challenge. Indeed, catalytic methods for C(*sp*³)-F bond formation are rare, and even when catalysis is achieved, other issues such as poor activity, low selectivity and/or factors associated with scalability – particularly recovery and reuse of the catalyst – are prevalent.

Amongst various enabling technologies,⁴ recent studies have demonstrated the potential of using light to facilitate fluorination chemistry, with Selectfluor® as fluorinating agent and homogeneous species as photocatalysts.⁵ Combining fluorination with photocatalysis (photofluorination) represents a very powerful and sustainable approach, and represents a major breakthrough for the field. However, several disadvantages are observed with these previous methods. For example, the reaction mechanisms predominating during such processes have not yet been clearly identified, prohibiting detailed structure-function relationships from guiding catalyst design. More critically, the photocatalysts developed to date also suffer from severe drawbacks, including the requirement for high loadings of scarcely available and/or prohibitively expensive metal centres (Ir, Ru), poor levels of intrinsic activity, and/or difficulties associated with their molecular complexity and homogeneous nature (recovery, reusability, scalability).⁵ Herein, we demonstrate that commercially available titanium dioxide, TiO₂, a non-toxic, stable and readily available semiconductor, can be efficiently employed as a heterogeneous photofluorination catalyst. When combined with the decarboxylative fluorination reaction – a powerful and sustainable method for C(*sp*³)-F bond synthesis⁶ – selective photofluorination of a variety of aliphatic carboxylic acids can be achieved under mild electrophilic fluorinating conditions. Under 365 nm irradiation, remarkable fluorine yields can be achieved in very short reaction times (< 10 minutes), resulting in turnover frequency (TOF) values over one order of magnitude larger than previously reported (1050 h⁻¹). The employment of water as solvent, the avoidance of scarce metals, and the facile recovery of TiO₂ - reused up to 4 times - also dramatically increase the sustainability of this method over alternative fluorination methods. Spectroscopic studies with Diffuse Reflectance Infrared

Fourier Transform (DRIFT) spectroscopy, Temperature Programmed Desorption Mass Spectrometry (TPD-MS), ^{19}F Magic Angle Spinning (MAS) NMR and X-Ray Photoelectron spectroscopy (XPS) are coupled to classical mechanistic studies and actinometry, allowing a preliminary reaction mechanism, in which a combination of TiO_2 -catalyzed steps and free-radical process combine, to be proposed.

Results and discussion

Photocatalytic fluorination. Amongst a range of well-known photosensitive materials, we identified that commercially available TiO_2 (P25) possessed high levels of activity for the decarboxylative fluorination of aliphatic carboxylic acids, such as 2,2-dimethylglutaric acid (DMGA, **1a**). Under classical decarboxylative conditions (25 °C, Selectfluor®, aqueous phase, SI Section 1, Scheme 1)⁶ rapid fluorination of water-soluble acids could be achieved when TiO_2 was irradiated by a solar light simulator, or a 365 nm LED torch. Under irradiation, selective mono-fluorination of DMGA to 4-fluoro-4 methyl pentanoic acid (4F4MPA, **1b**) was observed, in line with the radical-based mechanism recently reported for this reaction, for which tertiary positions exhibit much higher activity than primary and secondary ones.⁶ Rapid reaction rates were observed, with around 80% 4F4MPA yield achieved in only 5 minutes of reaction time, when 6.25 mol % of Ti, relative to the substrate, was employed (triangles, Figure 1 (Left)). Control reactions were also performed, in the absence of K_2CO_3 , TiO_2 and Selectfluor®. In the absence of the fluorinating agent, no 4F4MPA was observed. Furthermore, in the absence of TiO_2 or K_2CO_3 , much lower levels of activity were observed. These indicate the crucial role(s) played by the solid catalyst, the fluorine source and the base in the reaction network. To further study the effect of base, a number of kinetic experiments at different base loading was performed. Higher activity was observed at 1.16 equivalents of K_2CO_3 relative to DMGA (Figure 1 (Right)). Interestingly, with higher amount of base (2.32 equivalents), a decrease of reaction rate was observed. Notably, 4F4MPA selectivity > 95 % was observed in all reactions.



Scheme 1. Photocatalytic decarboxylative fluorination of 2,2-dimethylglutaric acid (DMGA, **1a**) to yield 4-fluoro-4 methyl pentanoic acid (4F4MPA, **1b**).

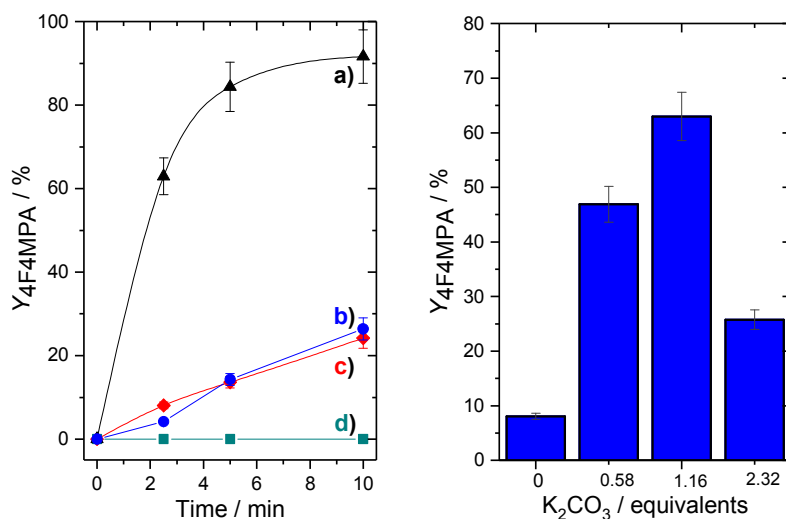


Figure 1 (Left). Yield of 4F4MPA (**1b**) with time over TiO₂ (P25) a) under standard conditions, b) in the absence of TiO₂, c) in the absence of K₂CO₃ and d) in the absence of Selectfluor®. **Figure 1 (Right).** Yield of 4F4MPA (**1b**) at 2.5 min with various amount of K₂CO₃ over TiO₂(P25). Standard reaction conditions: 0.2 mmol of DMGA (**1a**), 0.4 mmol of Selectfluor®, 0.0125 mmol TiO₂, 4 mL H₂O, 0.23 mmol K₂CO₃, N₂ atmosphere, 25 °C. Solar light simulator (300 W Xe arc lamp) was used to irradiate the reaction mixture.

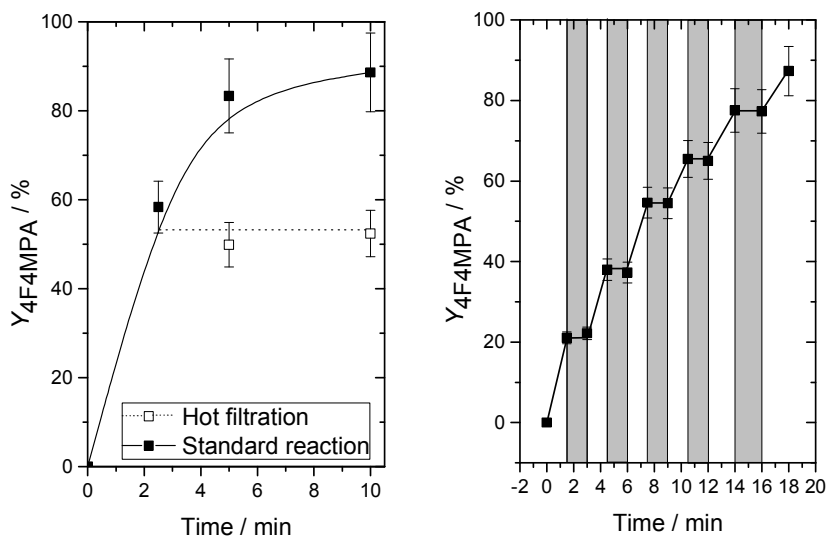
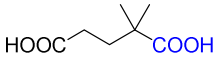
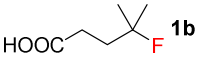
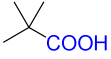
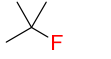
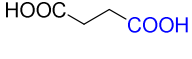
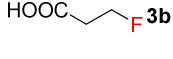
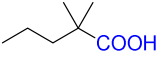
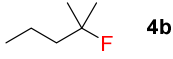
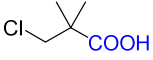
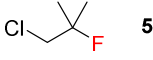
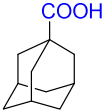
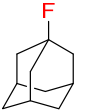
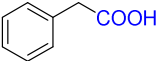
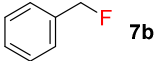


Figure 2 (Left). Solid line: Yield of 4F4MPA (**1b**) with time without filtering the catalyst. Dashed line, catalytic activity of the supernatant solution following filtration of the catalyst at 2.5 min. **Figure 2 (Right).** Yield of 4F4MPA (**1b**) with time over TiO₂ with light and (grey area) in dark conditions. Reaction conditions 1.0 mmol of DMGA (**1a**), 2.0 mmol of Selectfluor®, 0.0125 mmol TiO₂, 10 mL H₂O, 1.16 mmol K₂CO₃, N₂ atmosphere, 25 °C. Solar light simulator (300 W Xe arc lamp) was used to irradiate the reaction mixture.

To further optimize the reaction conditions, a number of experiments was performed at more challenging conditions. Excellent performance was still observed at 1.25 mol % of Ti, with the four-fold decrease in catalyst concentration (Figure 2 (Left)) resulting in TOF values of $1050 \pm 70 \text{ h}^{-1}$ being observed. Such values are an order of magnitude larger than those reported for any other photofluorination catalyst to date.^{5b} To ensure that the reaction is catalyzed heterogeneously, a hot filtration test was performed (SI Section 2). As can be seen (Figure 2 (Left)), removing TiO₂ at 2.5 minutes terminates the reaction, demonstrating catalysis to be heterogeneous. To verify the photocatalytic nature of the reaction, a light/dark experiment was performed, by periodically switching the lamp on and off (Figure 2 (Right)). Notably, no 4F4MPA formation occurred in the absence of light, confirming that constant irradiation is required for activity to be achieved.

Table 1. General applicability of TiO₂ for the photocatalytic fluorination of various carboxylic acids

Entry	Substrate	Product	Yield / % ^a
1	 1a	 1b	92, 35 ^b
2	 2a	 2b	94 ^c
3	 3a	 3b	48 ^d
4	 4a	 4b	42 ^e
5	 5a	 5b	46 ^{d,e}
6	 6a	 6b	22 ^e
7	 7a	 7b	17 ^{e,f}

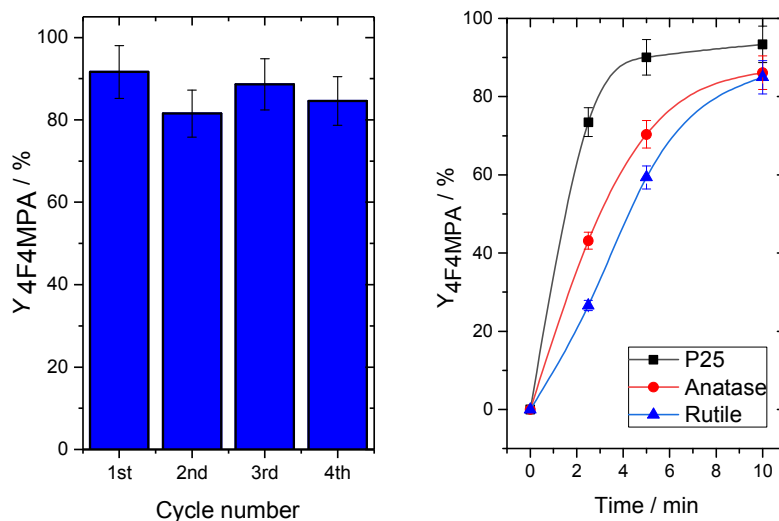
^aYields calculated as “mol (product)/mol (mol substrate) x 100” for entries 1, 3-7, and as “mol (**2a** converted)/mol(initial mol **2a**)” for entry 2 due to high product volatility. ^b2 mL H₂O and 2 mL of (CH₃)₂CO as solvent. ^c0.115 mmol K₂CO₃. ^dReaction time 30 min. ^e5 mL H₂O, 5 mL (CH₃)₂CO, 0.115 mmol K₂CO₃. ^fReaction time 60 min. Yields calculated with ¹⁹F NMR using α,α,α -trifluorotoluene and HPLC analysis against authentic standards. Reaction conditions: 0.2 mmol substrate, 0.4 mmol Selectfluor®, 0.0125 mmol TiO₂, 4 mL H₂O, 0.23 mmol of K₂CO₃, 25 °C, 10 min. Monochromatic LED irradiation of 365 nm was employed.

1 The general applicability of TiO₂ to photofluorinate carboxylic acids was also explored (Table 1, SI
2 Appendix Section). Interestingly, TiO₂ was also found to be able to photofluorinate primary carboxylic acids,
3 such as succinic acid, **3a**, and 2-phenylacetic acid, **7a**, albeit at lower levels of activity due to the greater
4 difficulty of forming primary alkyl radicals.⁷ Notably, TiO₂ was also able to photofluorinate non-water
5 soluble substrates, when a mixture of water/acetone was used as solvent.
6
7
8
9
10

11
12 One of the major advantages of heterogeneous catalysts over their homogeneous analogues is the
13 ease in which they can be recovered and reused, leading to increases in process sustainability and scalability.
14 Thus, the durability of TiO₂ to be used in successive cycles was also investigated, using DMGA as substrate
15 and neat water as reaction solvent (Figure 3 (Left), SI Section 3). Notably, the same final yield values were
16 achieved after 10 minutes in every catalytic cycle, for both fresh and used catalyst. Although a decrease in
17 reaction rate was observed following the first reuse of TiO₂ (SI Figure S1), no further decrease in
18 performance over successive cycles occurred *i.e.* the same kinetic performance was observed for the second,
19 third and fourth cycles. The ability to reuse the catalyst, without loss in maximum activity over extended
20 cycles, even in the absence of periodic regeneration treatments, is notable, and indicates the material
21 possesses potential for extended operation.⁸ Preliminary characterization of fresh and used catalyst, indicates
22 that although no change in surface area occurs during reaction (55 m² g⁻¹ for both fresh and used sample, SI
23 Table S1), conversion between the two crystalline phases present in P25, *i.e.* anatase and rutile, occurs to
24 some extent (SI Table S2). The relative ratio anatase:rutile was found to decrease slightly following each
25 catalytic cycle, going from a maximum of 86:14 for fresh TiO₂, to a ratio of 78:22, observed at the 4th
26 catalytic cycle. The small phase transformations observed, may, therefore, account for the slight decrease in
27 intrinsic kinetic activity.
28
29
30
31
32
33
34
35
36
37
38
39
40
41
42
43
44

45 To further investigate this, the photocatalytic activity of the two pure crystalline phases, *i.e.* anatase
46 and rutile, was investigated under the conditions previously employed for P25, using a monochromatic LED
47 torch at 365 nm (Figure 3 (Right)). As can be seen, lower levels of performance were exhibited by both pure
48 rutile and pure anatase, when compared to P25, in line with previous studies.⁹ Although this may arise from
49 reported synergistic effects, we stress that the poorer performance of both pure phases may also be related to
50 their different physical properties, such as surface area and crystallite size (SI Figures S2-3, Table S1-S3).⁹
51 Notably, different activity was also observed between anatase and rutile, with the latter being less active.
52
53
54
55
56
57
58
59
60

1
2 However, the higher levels of photocatalytic performance exhibited by anatase compared to rutile is in good
3 agreement to several previous reports.¹⁰
4
5
6
7



8
9
10
11
12
13
14
15
16
17
18
19
20
21
22
23
24
25
26
27 **Figure 3 (Left).** Reusability of TiO₂ with DMGA (**1a**) as substrate. No intermediate treatments were
28 performed between cycles. Reaction conditions otherwise identical to Figure 1. **Figure 3 (Right)** Yield of
29 4F4MPA (**1b**) with time over a) P25, b) anatase and c) rutile. Reaction conditions 0.2 mmol of DMGA (**1a**),
30 0.4 mmol of Selectfluor®, 0.0125 mmol TiO₂, 4 mL H₂O, 0.23 mmol K₂CO₃, N₂ atmosphere, 25 °C.
31 Forensic monochromatic LED torch at 365nm wavelength (Labino® Torch Light UVG2 Spotlight) was used
32 to irradiate the reaction mixture.
33
34
35

36
37
38
39 **Mechanistic studies.** Several potential chemical reactions can occur during photofluorination. Accordingly,
40 obtaining a detailed understanding of the reaction mechanism(s) is extremely challenging. Indeed, from the
41 literature a number of possible reaction mechanisms can be proposed, ranging from SET processes between
42 carboxylate groups bound on TiO₂,¹¹ to SET processes between radical alkyl species and Selectfluor®.¹²
43 Also, direct interactions between Selectfluor® and TiO₂ could result in formation of Ti-F intermediates,¹³
44 which may participate in the reaction mechanism. Thus, to gain preliminary insight into the potential
45 mechanism, a variety of spectroscopic experiments were performed.
46
47
48
49
50
51
52
53

54 To investigate interaction between the substrate and catalyst, DRIFT studies were performed. These
55 studies were performed on pivalic acid (**2a**, Table 1), a more volatile substrate than DMGA that also
56
57
58
59
60

undergoes decarboxylative photofluorination (Table 1). To first establish the nature of the interaction between pivalic acid/TiO₂ in the absence of light, pivalic acid was adsorbed on TiO₂ at 30 °C (Figure 4), and the sample was subsequently heated to 600 °C (Figure 5). After dosing the adsorbate at 30 °C, new features appear in the IR spectrum ((i), blue line, Figure 4); a group of bands in the region 3000-2850 cm⁻¹ characteristic of aliphatic C-H stretching, and other signals in the region 1700-1100 cm⁻¹. Interestingly, although the new C-H stretching bands correspond well to those observed for free *i.e.* non-adsorbed, pivalic acid ((ii), red line, Figure 4), the signal at 1692 cm⁻¹, characteristic of the key -COOH group ((ii), red line, Figure 4), only appears in low intensity, clearly demonstrating that only a negligible percentage of pivalic acid adsorbs onto the catalyst surface in its free acidic form. However, new vibrations in the region 1600-1100 cm⁻¹ are observed, consistent with those reported for deprotonated pivalic acid, (CH₃)₃CCOO⁻.¹⁴

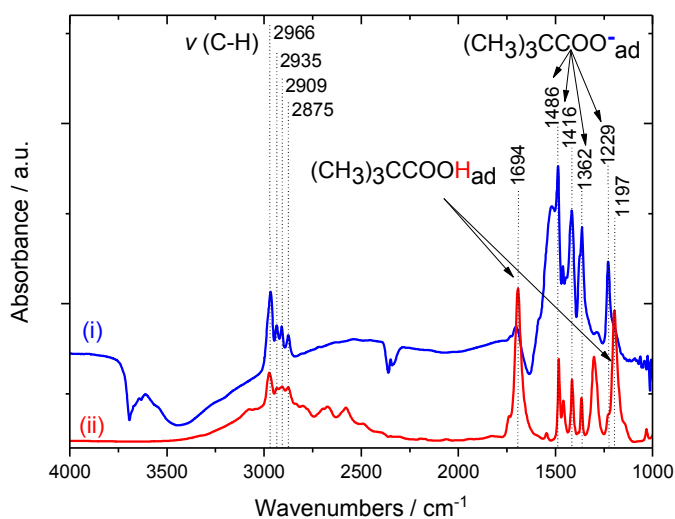
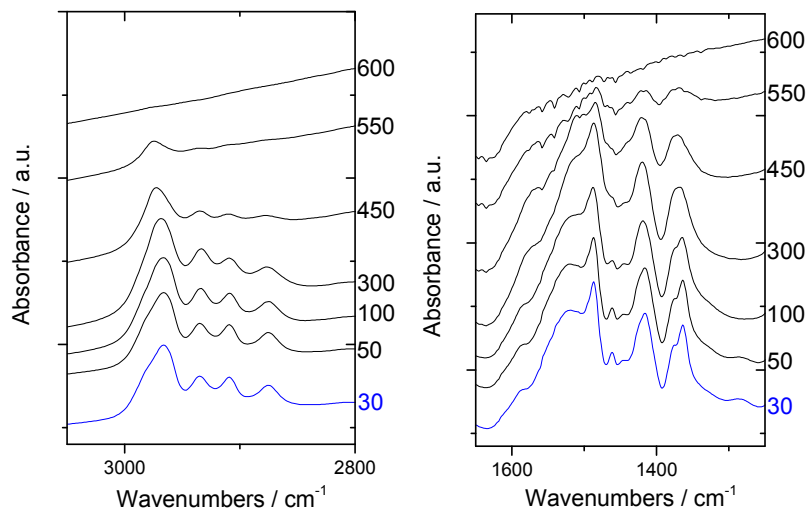


Figure 4. i) DRIFT spectra of TiO₂ after adsorption of pivalic acid (blue line) and ii) DRIFT spectra of free pivalic acid (red line).

The thermal stability of the adsorbed pivalic acid was subsequently explored by heating the DRIFT cell to various temperatures (Figure 5). Whilst the residual feature at 1692 cm⁻¹ disappears above 50 °C, indicating that the small quantities of pivalic acid in its acid form are merely physisorbed, the vibrations at 1600-1100 cm⁻¹, and the C-H stretching features at 3000-2850 cm⁻¹, are very stable during heat treatment. Indeed, all these peaks are still clearly visible at 300-450 °C, temperatures much higher than the boiling point of pivalic

1 acid (165 °C). Therefore, all the new features observed following interaction with TiO₂ can be assigned to a
2
3 strongly chemisorbed (CH₃)₃CCOO⁻ species (henceforth denoted as (RCOO⁻)_{ads}), indicating the formation of
4
5 an (RCOO⁻)TiO₂ intermediate.
6
7
8
9



10
11
12
13
14
15
16
17
18
19
20
21
22
23
24
25
26
27
28 **Figure 5.** Spectral changes observed to DRIFT spectra of TiO₂ after adsorption of pivalic acid at different
29 temperatures, from 30 °C (bottom line) to 600 °C (top line).
30
31
32
33

34 To evaluate the role of light during the reaction, and to verify the changes observed to the chemisorbed
35 (RCOO⁻)TiO₂ intermediate during photoirradiation, an experiment was performed whereby the DRIFT cell
36 containing the TiO₂-bound carboxylate species was irradiated with a monochromatic light of 365 nm
37 wavelength. Prior to irradiation, no decrease of the intensity of this species was observed over several hours
38 (SI Figure S4). Figure 6 presents the spectral changes that occur throughout the irradiation period. Upon
39 irradiation, a continuous decrease of intensity for all the features related to the (RCOO⁻)TiO₂ intermediate
40 were observed. This clearly indicates that pivalate decomposition occurs during the entire irradiation period.
41
42 Loss of the pivalate under these conditions likely results from its decomposition from R-COO⁻ into R[•] and
43
44 CO₂, as reported by Henderson *et al.* and Manley *et al.* for classical decarboxylative reactions.¹¹ Further
45
46 evidence of this mechanism was obtained through the observation of CO₂ in the effluent of a TPD-MS
47
48 experiment, following photoirradiation of DMGA-treated TiO₂ (SI Figure S5-9). Accordingly, DRIFTS and
49
50 TPD-MS studies indicates that the carboxylic acid groups of the substrate bind to the TiO₂ surface in their
51
52
53
54
55
56
57
58
59
60

1
2
3
4
5
6
7
8
9
10
11
12
13
14
15
16
17
18
19
20
21
22
23
24
25
26
27
28
29
30
31
32
33
34
35
36
37
38
39
40
41
42
43
44
45
46
47
48
49
50
51
52
53
54
55
56
57
58
59
60

carboxylate form, and only decompose from the surface under photoirradiation, accompanied by the loss of CO_2 .^{11,14}

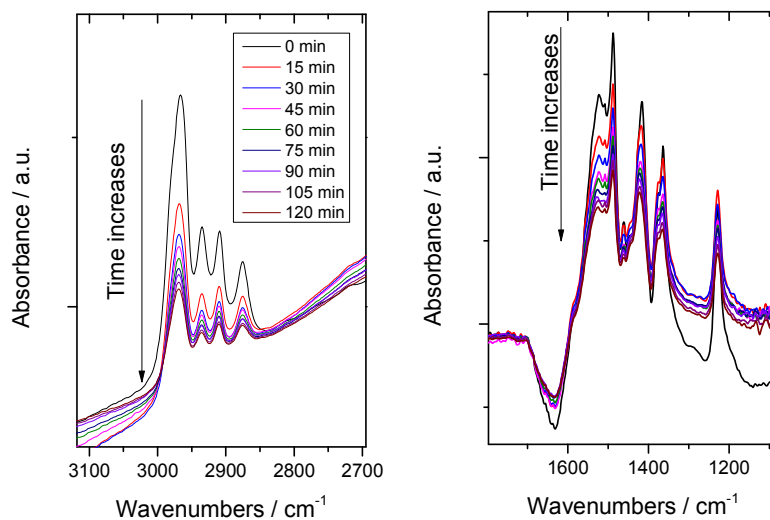


Figure 6. DRIFT spectra of TiO_2 -bound pivalate species, during irradiation with a monochromatic UV light of 365nm (Labino® Torch Light UVG2 Spotlight).

In addition to substrate/ TiO_2 interactions, the contribution of potential F/TiO_2 intermediates was also evaluated. Indeed, fluorination of TiO_2 surfaces, resulting in the formation of various Ti-F species, has been widely reported.¹³ To investigate the potential involvement of such species in the reaction mechanism, 300 mg of TiO_2 was treated with an aqueous solution of Selectfluor® under general reaction conditions, but in the absence of the substrate. Analysis of this sample by XPS revealed that following treatment, residual amounts of fluorine species (0.08 mmol g^{-1}) with a binding energy of 684.6 eV were found on the catalyst surface (SI Figure S10-14). ^{19}F MAS NMR analysis of the same sample (Figures S15-16) indicates the covalent nature of this interaction (henceforth denoted as F/TiO_2), in line with the previous report of Dambournet.¹⁵ Notably, these species were also observed on used catalysts (SI Figure S10, Table S4).

To investigate the potential role of F/TiO_2 , isolated samples containing this species were screened for reactivity, by performing the photofluorination of DMGA in the absence of other fluorinating agents, but

with F/TiO₂ present as catalyst. Although the catalyst containing a sufficient amount of fluorine to permit up to 80 % yield to be achieved, no conversion and no 4F4MPA yield were detected under the standard photofluorination conditions over a period of 30 minutes. This excludes the possibility of F/TiO₂ species acting as the active fluorinating species, and suggests that Selectfluor® containing active fluorine (F-TEDA, Figure 7) to be directly responsible for fluorine transfer. To allow proper discrimination amongst F-TEDA and its decomposition products, the following notations are adopted in the sections below.

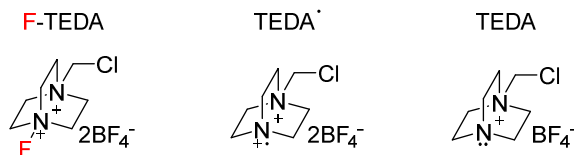


Figure 7. Schematic representation of F-TEDA and its subsequent decomposition products.

Following identification of F-TEDA as the active fluorine transfer agent, the stoichiometry of the decarboxylative fluorination reaction, in terms of F-TEDA consumed to 4F4MPA produced, was explored, by decreasing the amount of Selectfluor® from the 2 equivalents typically used under standard conditions, to 1 and 0.5 equivalents, respectively. When 1 and 0.5 equivalents were employed for DMGA decarboxylative fluorination, 4F4MPA yields up to 84% and 41% were achieved, respectively (Figure 8 (Left)). To better understand the stoichiometry, F-TEDA consumption was also measured at different reaction times via ¹⁹F NMR, by monitoring the disappearance of signal at $\delta = +48$ ppm (characteristic to the N-F bond) (SI Figure S17). This analysis confirmed that 1.2 equivalents are required for 1 equivalent of 4F4MPA to be produced, at the lowest F-TEDA concentrations (SI Tables S5-6). Notably, the initial reaction rate (*k*) measured at different starting concentrations of F-TEDA also demonstrated a linear dependence on the initial concentration of F-TEDA (SI Figures S18-19), indicating that F-TEDA is involved in the rate determining step of the reaction. However, the small excess of F-TEDA required (1.2 equivalents) also indicates that competitive reaction pathways, leading to passivation of F-TEDA, occur. This is in line with our previous findings (*Vide Supra*), involving the formation of inactive F/TiO₂ species, as observed by both XPS and ¹⁹F MAS NMR.

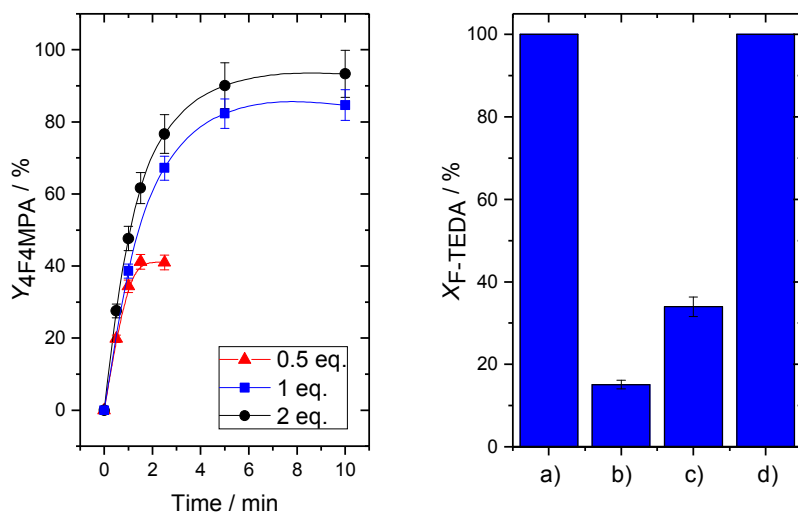


Figure 8 (Left). Yield of 4F4MPA (**1b**) with time over TiO_2 with i) 0.5 equivalents of Selectfluor®, 0.1 mmol (triangle), ii) 1 equivalent of Selectfluor®, 0.2 mmol (squares), iii) and 2 equivalents of Selectfluor®, 0.4 mmol (circles). Reaction conditions: 0.2 mmol of DMGA (**1a**), various amounts of Selectfluor®, 0.0125 mmol TiO_2 , 4 mL H_2O , 0.23 mmol K_2CO_3 , 25 °C, N_2 . Forensic monochromatic LED torch at 365 nm wavelength (Labino® Torch Light UVG2 Spotlight) was used to irradiate the reaction mixture. **Figure 8 (Right).** Conversion of F-TEDA at 10 min a) under standard conditions, b) under standard conditions but without TiO_2 , c) under standard conditions but without K_2CO_3 , and d) under standard conditions but without DMGA (**1a**).

The consumption of F-TEDA may occur from several processes, such as: i) general instability under the aqueous environment, ii) selective consumption as a consequence of reaction, *i.e.* following attack by the alkyl radical R^\cdot , iii) non-selective interactions with the base, and iv) non-selective interactions with TiO_2 *i.e.* F/ TiO_2 formation. In order to investigate the extent of these pathways, the amount of F-TEDA converted at 10 minutes was monitored under otherwise-standard reaction reactions but: i) in the absence of TiO_2 , ii) in the absence of K_2CO_3 , and iii) in the absence of the substrate, DMGA (**1a**) (Figure 8 (Right)). Interestingly, complete conversion of F-TEDA was observed even in the absence of the substrate, when both TiO_2 and K_2CO_3 were present, indicating that F-TEDA can be converted even in the absence of substrate. However, in the absence of either TiO_2 or K_2CO_3 , much lower levels of F-TEDA were converted. In addition to

1 confirming the essential role of TiO_2 in catalyzing all stages of the reaction, this observation suggests that in
2 addition to being required to deprotonate the substrate, favoring the formation of the $(\text{R-COO}^-)\text{TiO}_2$
3 intermediate, an additional role of K_2CO_3 in the reaction mechanism may be to act as sacrificial electron
4 donor (*i.e.* hole scavenger), favoring charge separation e^-/h^+ in photoactivated TiO_2 .¹⁶ This may account for
5 the observation that the optimal amount of K_2CO_3 is just over 1 equivalent, relative to DMGA (Figure 1
6 (Right)). In the absence of substrate, TiO_2 and K_2CO_3 , no F-TEDA was consumed, pointing to its otherwise
7 stable nature under the general reaction conditions. Additional experiments performed replacing K_2CO_3 with
8 a strong Brønsted-Lowry base, NaOH (SI Figure S20), indicates that, although good catalytic performances
9 are still observed in the presence of NaOH, higher catalytic activity is achieved in the presence of K_2CO_3 .
10 This may be due to the ability of the carbonate species to consume the photo-generated holes (h^+), forming
11 carbonate radicals.
12
13
14
15
16
17
18
19
20
21
22
23

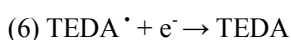
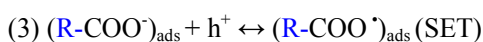
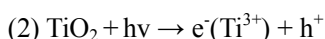
24 Considering the radical nature of several species involved in the reaction mechanism, the effect of
25 O_2 , a well known alkyl radical scavenger, was also investigated.¹⁷ Performing the reaction in O_2 , as opposed
26 to N_2 , resulted in a decrease in 4F4MPA yield (SI Figure S21). The decrease in 4F4MPA in the presence of
27 O_2 implies that alkyl radicals may be involved in the rate determining step. This is in line with the known
28 ability of O_2 to trap carbon-centered radicals, hence prohibiting the introduction of fluorine.¹⁶
29
30
31
32
33
34
35
36
37

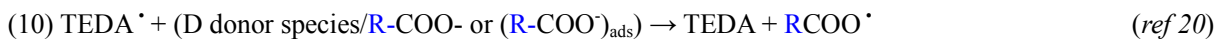
38 **Identifying the photocatalytic properties of the system.** In photocatalysis, the number of photons
39 efficiently employed in a chemical process, is one of the key parameters to describe the efficiency of the
40 system, allowing proper comparison with other existing photocatalytic systems. Therefore, the apparent
41 number of photons efficiently employed (“*apparent photon efficiency*, ξ ”) for decarboxylative fluorination
42 under reaction conditions was measured by calculating the ratio between the number of molecules converted
43 over time versus the number of incident photons under the same period of time. It is noteworthy to mention
44 that in heterogeneous catalysis it is important to discriminate between the number of incident photons and
45 the number of photons efficiently absorbed by the solid catalyst and the term quantum yield, Φ , (or quantum
46 efficiency) can be correctly employed only as a function of the number of photons actually absorbed by the
47 catalyst.¹⁸
48
49
50
51
52
53
54
55
56
57
58
59
60

$$\xi = \frac{\text{molecules of substrate converted}}{\text{number of incident photons}} \quad \Phi = \frac{\text{molecules of substrate converted}}{\text{number of absorbed photons}}$$

Considering that the number of incident photons is always higher than the number of photons absorbed by the heterogeneous material, ξ is always lower than the quantum yield, Φ , of the system. However, ξ may still be used to investigate if light behaves as a true catalyst (ξ greater than 1) or not (photosensitized process), even though it does not give real information on the quantum yield of the system. To investigate the catalytic properties of light in the system, the photon flow through the aqueous reaction mixture was determined using a standard ferrioxalate actinometry method,¹⁹ under 365 nm light irradiation (SI Figures S22-23). Under these conditions, a photon flow of $(2.0 \pm 0.5) \times 10^{17}$ photons/s was measured. This value was then used to measure the “apparent photon efficiency” of the system as a ratio between the number of molecules of DMGA converted (at 30 and 60 seconds) and the number of incident photons (photon flow * 30 and 60 seconds, respectively), giving an “apparent photon efficiency” of 3.5 ± 0.5 . An apparent photon efficiency greater than 1 implies an even higher quantum efficiency of the system, thus indicating that light is a true catalyst for this reaction, with one absorbed photon being able to catalyze more than 1 catalytic cycle. This further suggests that a free radical chain mechanism dominates, contributing to the overall reaction mechanism, although light and TiO₂ are both essential for the catalytic activity to be observed. Preliminary investigation into the effect of the intensity of the light on the reaction rate was also performed, showing correlation between the intensity of the light source and the reaction rate (SI Figure S24). The observation of the catalytic nature of light in the system further demonstrates the high levels of sustainability exhibited by this system, relative to classical methods of fluorination.

Overall reaction mechanism. Based on all the observations described above, an overall reaction mechanism can be proposed:





5
6
7
8
9
10 DRIFT analysis indicates that carboxylic acids bind to the TiO_2 surface in their carboxylate form (1).¹⁴ This
11 may account for the poor catalytic performances observed exhibited by TiO_2 when K_2CO_3 is not present in
12 the reaction mixture. Simultaneously to substrate adsorption, photoexcitation of TiO_2 with UV light leads to
13 the formation of electron-hole pairs (2). The positive holes (h^+) so generated, can subsequently withdraw an
14 electron from the chemisorbed carboxylate species according to the photo-Kolbe reaction,²¹ *via* SET leading
15 to the generation of radical species R-COO^\bullet (3). These radicals can then decompose (β -scission) to yield CO_2
16 (observed by TPD-MS in the absence of Selectfluor®) and alkyl radical species R^\bullet (4). The presence of R^\bullet is
17 inferred from the radical nature of the reaction (apparent photon efficiency greater than 1), and the negative
18 role exhibited by O_2 in the system.¹⁷ Alternatively, R-COO^\bullet species can also further react with TiO_2 *via*
19 additional SET, re-establishing the R-COO^- species. Since it is known that F-TEDA ($E^0 = -0.296$ V vs.
20 Ag/Ag^+ electrode)²² is able to functionalise such radical substrates through SET, we hypothesise that
21 following decarboxylation, the alkyl radical species, R^\bullet , reacts with F-TEDA, resulting in the formation of
22 the desired R-F product, and an equivalent of the radical TEDA^\bullet (5). Notably, the radical species TEDA^\bullet , can
23 subsequently trap the free electron released by photoexcitation of TiO_2 , resulting in the more stable species
24 TEDA , in analogy to the mechanism proposed by the MacMillan group for Ir-photocatalyzed
25 decarboxylative fluorination (6).^{5a} Reaction step (7) can also occur, resulting in the formation of F/ TiO_2
26 species (confirmed by XPS and ^{19}F MAS NMR), accounting for the excess of F-TEDA required for the
27 reaction (DMGA : F-TEDA stoichiometry of 1 : 1.2) with formation of the radical species TEDA^\bullet . The
28 ability of F/ TiO_2 species to undergo to fluorine transfer was also investigated (8), however, mechanistic
29 studies confirmed that reaction step (8) can be discounted from contributing to the catalytic mechanism (*Vide*
30 *Supra*), with F/ TiO_2 species found to be inactive. The excess of holes (h^+) formed by reaction step (7)
31 explains the requirement for an excess of K_2CO_3 (optimal amount found to be 1.2 eq.), which, in addition to
32 deprotonating the substrate, is also a well-known hole scavenger, acting as a sacrificial electron donor
33 (reaction step (9)).¹⁶

In addition to this main catalytic cycle (Figure 9), another free radical pathway (blue arrow, pathway ii, Figure 9), initiated by the main catalytic cycle, may occur, accountable for the apparent photon efficiency greater than 1 (*Vide Supra*). The radical TEDA[•] formed in reaction steps (5) and (7), in addition to withdrawing an electron from TiO₂ (6) (pathway i, Figure 9), may also react with other electron donor species present in the reaction systems,²⁰ such as carboxylate ions (R-COO⁻) or adsorbed (R-COO⁻)_{ads}, according to reaction step (10) (pathway ii, blue arrow, Figure 9), yielding to the carboxyl radical RCOO[•] species. The new formed carboxyl radical species RCOO[•], can then decompose, according to reaction step (4), yielding CO₂ and alkyl radical R[•], further reacting with another molecule of F-TEDA, closing the second cycle, accountable to the greater than one photon efficiency previously measured with the actinometry. Despite the presence of multiple pathways, light and TiO₂ remain an essential component of the system, since none of the catalytic cycles can be closed in their absence. This accounts for the catalytic nature of TiO₂ *i.e.* the observation that no reaction occurs in its absence, and the fact catalytic activity ceases in the absence of light (Figure 2 (Right)). Moreover, the overall stoichiometry between F-TEDA and 4F4MPA remains approximately 1:1.

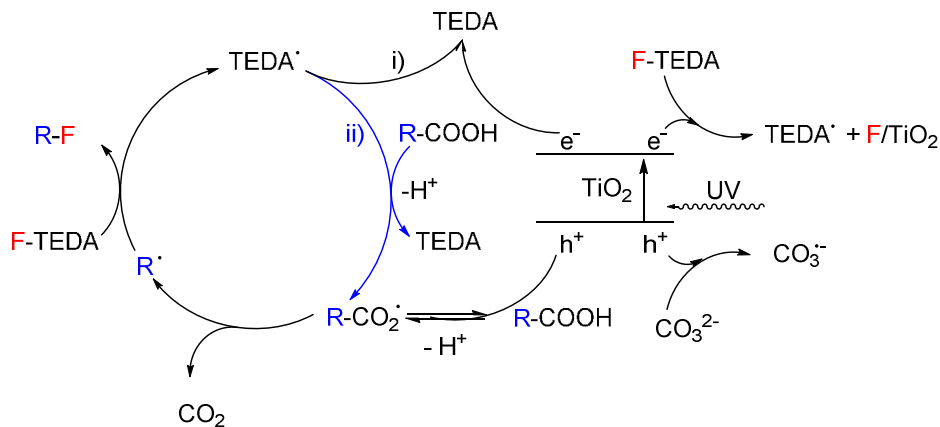


Figure 9. Proposed reaction mechanism for TiO₂ photocatalyzed decarboxylative fluorination of aliphatic carboxylic acids.

Conclusions.

In this work, commercially available TiO₂ (P25) is found to be an efficient and reusable heterogeneous photocatalyst for the decarboxylative fluorination of various carboxylic acids in aqueous media at 25°C, with

1 electrophilic fluorine reagents (Selectfluor®). The high TOFs values observed (up to $1050 \pm 70 \text{ h}^{-1}$), as well
2 as the ease of recovery and reusability of this material (up to 4 catalytic cycles reported here), confer to this
3 method higher sustainability than any fluorination system reported in literature, in addition to increased
4 potential for scale up. Spectroscopic and mechanistic studies performed on this system indicate the presence
5 of a complex reaction network, in which a combination of surface-catalyzed steps and free-radical process
6 combine to result in exceptional levels of activity, both in terms of yield and selectivity, but also in photon
7 efficiency.
8
9
10
11
12
13
14
15
16
17

18 **Experimental Section**

19
20 All experimental details are provided in the Supporting Information.
21
22
23

24 **Supporting Information.**

25
26 Supporting information containing all kinetic, spectroscopic, experimental and product characterization
27 details (NMR, HPLC) is provided.
28
29
30
31
32

33 **Acknowledgements**

34
35 CH gratefully appreciates financial support from The Royal Society through provision of a University
36 Research Fellowship (UF140207). CH and GT acknowledge The Royal Society for additional research
37 funding (CH160135). Luca Botti (DRIFTS), Davide Motta (XPS) and Dr. David Apperley (MAS NMR) are
38 thanked for additional experimental input.
39
40
41
42
43
44
45
46

47 **References**

- 48
49 (1) (a) Müller, K.; Faeh C.; Diederich, F. Fluorine in Pharmaceuticals: Looking Beyond Intuition. *Science*
50 **2007**, *317*, 1881-1886. (b) O'Hagan, D. Understanding Organofluorine Chemistry. An Introduction to
51 the C-F Bond. *Chem. Soc. Rev.* **2008**, *37*, 308-319. (c) Liang, T.; Neumann C. N.; Ritter, T. Introduction
52 of Fluorine and Fluorine-Containing Functional Groups. *Angew. Chem. Int. Ed.* **2013**, *52*, 8214-8264.
53 (d) Purser, S.; Moore, P. R.; Swallow S.; Gouverneur, V. Fluorine in Medicinal Chemistry. *Chem. Soc.*
54 *Rev.* **2008**, *37*, 320-330. (e) Ritter, T. Catalysis: Fluorination Made Easier. *Nature* **2010**, *466*, 447-448.
55
56
57
58
59
60

- 1
2
3
4
5
6
7
8
9
10
11
12
13
14
15
16
17
18
19
20
21
22
23
24
25
26
27
28
29
30
31
32
33
34
35
36
37
38
39
40
41
42
43
44
45
46
47
48
49
50
51
52
53
54
55
56
57
58
59
60
- (2) (a) Miller, P. W.; Long, N. J.; Vilar R.; Gee, A. D. Synthesis of ^{11}C , ^{18}F , ^{15}O and ^{13}N Radiolabels for Positron Emission Tomography. *Angew. Chem. Int. Ed.* **2008**, *47*, 8998-9033. (b) Littich R.; Scott, P. J. H. Novel Strategies for Fluorine-18 Radiochemistry. *Angew. Chem. Int. Ed.* **2012**, *51*, 1106-1109. (c) Brooks, A. F.; Topczewski, J. J.; Ichiishi, N.; Sanford M. S.; Scott, P. J. H. Late-stage [^{18}F] Fluorination: New Solutions to Old Problems. *Chem. Sci.* **2014**, *5*, 4545-4553.
- (3) (a) Liu, W.; Huang, X.; Cheng, M. J.; Nielsen, R. J.; Goddard III W. A.; Groves, J. T. Oxidative Aliphatic C-H Fluorination with Fluoride Ion Catalyzed by a Manganese Porphyrin. *Science* **2012**, *337*, 1322-1325. (b) Sibi M. P.; Landais, Y. C(sp³)-F Bond Formation: a Free-Radical Approach. *Angew. Chem. Int. Ed.* **2013**, *52*, 3570-3572. (c) Furuya, T.; Kamlet A. S.; Ritter, T. Catalysis for Fluorination and Trifluoromethylation. *Nature* **2011**, *473*, 470-477. (d) Liu, W.; Groves J. T. Manganese-Catalyzed Oxidative Benzylic C-H fluorination by Fluoride Ions. *Angew. Chem., Int. Ed.* **2013**, *52*, 6024-6027. (e) Hull, K. L.; Anani W. Q.; Sanford, M. S. Palladium-Catalyzed Fluorination of Carbon-Hydrogen Bonds. *J. Am. Chem. Soc.* **2006**, *128*, 7134-7135. (f) Watson, D. A.; Su, M.; Teverovskiy, G.; Zhang, Y.; Garcia-Fortanet, J.; Kinzel T.; Buchwald, S. L. Formation of ArF from LPdAr(F): Catalytic Conversion of Aryl Triflates to Aryl Fluorides. *Science* **2009**, *325*, 1661-1664. (g) Hickman A. J.; Sanford, M. S. High-Valent Organometallic Copper and Palladium in Catalysis. *Nature* **2012**, *484*, 177-185.
- (4) (a) Howard, J. L.; Sagatov, Y.; Repousseau, L.; Schotten, C.; Browne, D. L. Controlling Reactivity Through Liquid Assisted Grinding: The Curious Case of Mechanochemical Fluorination. *Green Chem.* **2017**, *19*, 2798-2802. (b) Wang, Y.; Wang, H.; Jiang, Y.; Zhang, C.; Shao, J.; Xu, D. Fast, Solvent-Free and Highly Enantioselective Fluorination of β -Keto Esters Catalyzed by Chiral Copper Complexes in a Ball Mill. *Green Chem.* **2017**, *19*, 1674-1677.
- (5) (a) Ventre, S.; Petronijevic, F. R.; MacMillan, D. W. C. Decarboxylative Fluorination of Aliphatic Carboxylic Acids via Photoredox Catalysis. *J. Am. Chem. Soc.* **2015**, *137*, 5654-5657. (b) Porras, J. A.; Mills, I. N.; Transue, W. J.; Bernhard, S. Highly Fluorinated Ir(III)-2,2':6',2''-Terpyridine-Phenylpyridine-X Complexes via Selective C-F Activation: Robust Photocatalysts for Solar Fuel Generation and Photoredox Catalysis. *J. Am. Chem. Soc.* **2016**, *138*, 9460-9472. (c) Rueda-Becerril, M.; Mahé, O.; Drouin, M.; Majewski, M. B.; West, J. G.; Wolf, M. O.; Sammis, G. M.; Paquin, J.-F. Direct C-F Bond Formation Using Photoredox Catalysis. *J. Am. Chem. Soc.* **2014**, *136*, 2637-2641. (d) Kee, C. W.; Chin, K. F.; Wong M. W.; Tan, C.-H. Selective Fluorination of Alkyl C-H Bonds via Photocatalysis. *Chem. Commun.* **2014**, *50*, 8211-8214. (e) Wu, X.; Meng, C.; Yuan, X.; Jia, X.; Qian, X.; Ye, J. Transition-Metal-Free Visible-Light Photoredox Catalysis at Room Temperature for Decarboxylative Fluorination of Aliphatic Carboxylic Acids by Organic Dyes. *Chem. Commun.* **2015**, *51*, 11864-11867. (f) West, J. G.; Bedell, T. A.; Sorensen E. J. The Uranyl Cation as a Visible-Light Photocatalyst for C(sp³)-H Fluorination. *Angew. Chem. Int. Ed.* **2016**, *55*, 8923-8927. (g) Neumann, C. N.; Ritter T. C-H Fluorination: U Can Fluorinate Unactivated Bonds. *Nat. Chem.* **2016**, *8*, 822-823. (h) Leung, J. C. T.; Chatalova-Sazepin, C.; West, J. G.; Rueda-Becerril, M.; J.-F. Paquin, J.-F.; Sammis, G. M. Photo-fluorodecarboxylation of 2-Aryloxy and 2-Aryl Carboxylic Acids. *Angew. Chem. Int. Ed.*, **2012**, *51*,

- 10804-10807. (i) Bloom, S.; Pitts, C. R.; Miller, D. C.; Haselton, N.; Holl, M. G.; Urheim, E.; Lectka, T. A Polycomponent Metal-Catalyzed Aliphatic, Allylic, and Benzylic Fluorination. *Angew. Chem. Int. Ed.* **2012**, *51*, 10580–10583. (j) Pitts, C. R.; Bloom, S.; Woltornist, R.; Auvenshine, D. J.; Ryzhkov, L. R.; Siegler, M. A.; Leckta, T. Direct, Catalytic Monofluorination of sp³ C–H Bonds: A Radical-Based Mechanism with Ionic Selectivity. *J. Am. Chem. Soc.* **2014**, *136*, 9780-9791. (k) Bloom, S.; McCann, M.; Lectka, T. Photocatalyzed Benzylic Fluorination: Shedding “Light” on the Involvement of Electron Transfer. *Org. Lett.* **2014**, *16*, 6338–6341.
- (6) Yin, F.; Wang, Z.; Li, Z.; Li, C. Silver-Catalyzed Decarboxylative Fluorination of Aliphatic Carboxylic Acids in Aqueous Solution. *J. Am. Chem. Soc.* **2012**, *134*, 10401-10404.
- (7) Blanksby, S. J.; Ellison, G. B. Bond Dissociation Energies of Organic Molecules. *Acc. Chem. Res.* **2003**, *36*, 255-263.
- (8) Hammond, C. Intensification studies of Heterogeneous Catalysts: Probing and Overcoming Catalyst Deactivation During Liquid Phase Operation. *Green. Chem.* **2017**, *12*, 2711-2728.
- (9) Su, R.; Bechstein, R.; Sør, L.; Vang, R. T.; Sillassen, M.; Esbjörnsson, B.; Palmqvist, A.; Besenbacher, F. How the Anatase-to-Rutile Ratio Influences the Photoreactivity of TiO₂. *J. Phys. Chem. C.* **2011**, *115*, 24287-24292.
- (10) Luttrell, T.; Halpegamage, S.; Tao, J.; Kramer, A.; Sutter, E.; Batzill, M. Why is Anatase a Better Photocatalyst Than Rutile? – Model Studies on Epitaxial TiO₂ Films. *Sci. Rep.* **2014**, *4*, 4043.
- (11) (a) Henderson, M. A.; White, J. M.; Uetsuka, H.; Onishi, H. Photochemical Charge Transfer and Trapping at the Interface Between an Organic Adlayer and an Oxide Semiconductor. *J. Am. Chem. Soc.* **2003**, *125*, 14974-14975. (b) Manley, D. W.; McBurney, R. T.; Miller, P.; Walton, J. C. Titania-Promoted Carboxylic Acid Alkylations of Alkenes and Cascade Addition-Cyclizations. *J. Org. Chem.* **2014**, *79*, 1386-1398.
- (12) Rueda-Becerril, M.; Chatalova Sazepin, C.; Paquin, J.; Sammis, G. Fluorine Transfer to Alkyl Radicals. *J. Am. Chem. Soc.* **2012**, *134*, 4026-4029.
- (13) (a) Sun, H.; Wang, S.; Ang, H. M.; Tadé, M. O.; Li, Q. Halogen Element Modified Titanium Dioxide for Visible Light Photocatalysis. *Chem. Eng. J.* **2010**, *162*, 437-447. (b) Moss, J. H.; Parfitt, G. D.; Wright, A. The Fluorination of Titanium Dioxide Surfaces. *Colloid Polym. Sci.* **1978**, *256*, 1121-1130. (c) Shifu, C.; Yunguang, Y.; Wei, L. Preparation, Characterization and Activity Evaluation of TiN/F-TiO₂ Photocatalyst. *J. Hazard. Mater.* **2011**, *186*, 1560-1567.
- (14) (a) Wen, B.; Li, Y.; Chen, C.; Ma, W.; Zhao, J. An Unexplored O₂-Involved Pathway for the Decarboxylation of Saturated Carboxylic Acids by TiO₂ Photocatalysis: An Isotopic Probe Study. *Chem. Eur. J.* **2010**, *16*, 11859-11866. (b) Backes, M. J.; Lukaski, A. C.; Muggli, D. S. Active Sites and Effects of H₂O and Temperature on the Photocatalytic Oxidation of ¹³C-Acetic Acid on TiO₂. *Appl. Catal. B-Environ.* **2005**, *61*, 21-35. (c) Szabó-Bárdos, E.; Baja, B.; Horváth, E.; Horváth, A. Photocatalytic Decomposition of L-Serine and L-Aspartic Acid Over Bare and Silver-Deposited TiO₂. *J. Photoch. Photobio. A* **2010**, *213*, 37-45.

- 1
2
3
4
5
6
7
8
9
10
11
12
13
14
15
16
17
18
19
20
21
22
23
24
25
26
27
28
29
30
31
32
33
34
35
36
37
38
39
40
41
42
43
44
- (15) (a) Li, W.; Body, M.; Legein, C.; Dambournet, D. Identify OH Groups in TiOF₂ and their Impact on the Lithium Intercalation Properties. *J. Sol. State Chem.* **2017**, *246*, 113-118. (b) Li, W.; Body, M.; Legein, C.; Borkiewicz, O. J.; Dambournet, D. Atomic Insights into Nanoparticle Formation of Hydroxyfluorinated Anatase Featuring Titanium Vacancies. *Inorg. Chem.* **2016**, *55*, 7182-7187. (c) Li, W.; Body, M.; Legein, C.; Dambournet, D. Sol-Gel Chemistry of Titanium Alkoxide Toward HF: Impacts of Reaction Parameters. *Cryst. Growth Des.* **2016**, *16*, 5441-5447.
- (16) Dimitrijevic, N. M.; Vijayan, B. K.; Poluektov, O. G.; Rajh, T.; Gray, K. A.; He, H.; Zapol, P. Role of Water and Carbonates in Photocatalytic Transformation of CO₂ to CH₄ on Titania. *J. Am. Chem. Soc.* **2011**, *133*, 3964-3971.
- (17) Maillard, B.; Ingold, K. U.; Scaiano J. C. Rate Constants for the Reactions of Free Radicals with Oxygen in Solution. *J. Am. Chem. Soc.* **1983**, *105*, 5095-5099.
- (18) Serpone, N.; Salinaro, A. Terminology, Relative Photonic Efficiencies and Quantum Yields in Heterogeneous Photocatalysis. Part 1: Suggested Protocol. *Pure & Appl. Chem.* **1999**, *71*, 303-320.
- (19) (a) Hatchard, C. G.; Parker, C. A. A New Sensitive Chemical Actinometer – II. Potassium Ferrioxalate as a Standard Chemical Actinometer. *Proc. R. Soc. London, Ser. A* **1956**, *235*, 518-536. (b) Su, R.; Dimitratos, N.; Liu, J.; Carter, E.; Althahban, S.; Wang, X.; Shen, Y.; Wendt, S.; Wen, X.; Niemantsverdriet J. W.; Iversen, B. B.; Kiely, C. J., Hutchings, G. J.; Besenbacher, F. Mechanistic Insight into the Interaction Between a Titanium Dioxide Photocatalyst and PdI Cocatalyst for Improved Photocatalytic Performance. *ACS Catal.* **2016**, *6*, 4239-4247.
- (20) Lantaño, B.; and Postigo, L. Radical Fluorination Reactions by Thermal and Photoinduced Methods. *Org. Biomol. Chem.* **2017**, *15*, 9954-9973.
- (21) (a) Kraeutler, B.; Bard, A. J. Heterogeneous Photocatalytic Synthesis of Methane from Acetic Acid – ne Kolbe Reaction Pathway. *J. Am. Chem. Soc.* **1978**, *100*, 2239-2240. (b) Kraeutler, B.; Bard, A. J. Photoelectrosynthesis of Ethane From Acetate Ion at an N-Type Titanium Dioxide Electrode. The Photo-Kolbe Reaction. *J. Am. Chem. Soc.* **1977**, *99*, 7729-7731.
- (22) Oliver, E. W.; Evans, D. H. Electrochemical Studies of Six N-F Electrophilic Fluorinating Reagents. *J. Electroanal. Chem.* **1999**, *474*, 1-8.

45 Table of Contents Graphic

